Strong-coupling-expansion analysis of the false-vacuum decay rate of the lattice ϕ^4 model in 1 + 1 dimensions

2001 J. Phys. A: Math. Gen. 34 11215

(http://iopscience.iop.org/0305-4470/34/50/304)

INSTITUTE OF PHYSICS PUBLISHING JOURNAL OF PHYSICS A: MATHEMATICAL AND GENERAL

J. Phys. A: Math. Gen. **34** (2001) 11215–11223 PII: S0305-4470(01)27634-3

Strong-coupling-expansion analysis of the false-vacuum decay rate of the lattice ϕ^4 model in 1 + 1 dimensions

Yoshihiro Nishiyama

Department of Physics, Faculty of Science, Okayama University, Okayama 700-8530, Japan

E-mail: nisiyama@psun.phys.okayama-u.ac.jp

Received 31 July 2001, in final form 15 October 2001
Published 7 December 2001
Online at stacks.iop.org/JPhysA/34/11215

Abstract

Strong-coupling expansion is performed for the lattice ϕ^4 model in 1 + 1 dimensions. Because the strong-coupling limit itself is not solvable, we employed numerical calculations so as to set up unperturbed eigensystems. Restricting the number of Hilbert-space bases, we performed linked-cluster expansion up to 11th order. We carried out an alternative simulation by means of the density-matrix renormalization group. Thereby, we confirmed that our series-expansion data with a convergence-acceleration trick are in good agreement with the simulation result. Through the analytic continuation to the domain of negative biquadratic interaction, we obtain the false-vacuum decay rate. Contrary to common belief that the tunnelling phenomenon lies out of perturbative treatments, our series expansion reproduces the instanton-theory behaviour for a high potential barrier. For a shallow barrier, in contrast, our result tells us that the relaxation is no longer described by an instanton, but the decay rate acquires notable enhancement.

PACS numbers: 64.60.My, 03.65.Xp, 12.38.Cy, 78.20.Bh

1. Introduction

Suppose that a system is placed in a certain metastable state surrounded by a local potential minimum, the system would be unstable to decay to a global minimum assisted by either quantum or thermal fluctuations. Such processes are called false-vacuum decay and metastability relaxation and they are considered to be non-perturbative in nature. Hence, in order to calculate the decay rate (lifetime), ingenious treatments have been invented so far [1–4]. Those treatments rely on the semiclassical approximation. That is, the treatments take into account the quadratic fluctuations around the field configuration which extremizes the Euclidean action. Such field configurations are called instanton, bounce and (critical) droplet.

Therefore, these treatments, just like the WKB approximation in wave mechanics, are not justified for strong fluctuations (namely, short lifetime). In addition, it is quite cumbersome to improve the approximation systematically.

In order to compensate for the above drawback, a first-principles calculation scheme free from any biased errors would be desirable. As for the discrete variable model (kinetic Ising model), actually, a remarkable *tour de force* scheme was invented by Günther *et al* [5]. They introduced the so-called constrained-transfer-matrix method, which meets the non-equilibrium situation. Then, they carried out extensive numerical calculations of the transfer matrix. In consequence, they extracted the imaginary part of the free energy, which is to be identified as the decay rate. To the best of our knowledge, it is the first *ab initio* approach to the decay rate in the presence of many-body correlations. Their result supports the aforementioned analytic theory based on the droplet picture. (Besides this, Monte Carlo simulation has been utilized to evolve the relaxation processes [6, 7], where the number of Monte Carlo steps is interpreted as the time progression. Though the interpretation is, in a strict sense, not fully justified, the simulation result is fairly in accordance with the droplet picture.)

In contrast, as for a continuous-variable model such as the ϕ^4 model, the above approach does not apply, and so far, no attempt at *ab initio* calculation has been reported. For the quantum-mechanics level (0 + 1 dimension), however, substantial progress has made [11]: Suzuki and Yasuta obtained a compact expression for the decay (tunnelling) rate based on the weak-coupling expansion and succeeding Borel resummation [12, 13]. They succeeded in calculating the tunnelling rate beyond instanton calculus. Alternatively, from the weak-coupling expansion, Karrlein and Kleinert obtained, remarkably enough, strong-coupling series by means of the so-called variational perturbation [14]. Both approaches pursue a first-principles calculation scheme beyond instanton calculus. As a consequence, these theories clarified how the instanton description fails for a low potential barrier; the true decay rate is suppressed owing to inter-instanton interaction. At present, extension to the many-body case appears to be unsuccessful [13].

The aim of this paper is to investigate the false-vacuum decay rate for many-body system through series expansion. We studied the lattice ϕ^4 model in 1 + 1 dimensions,

$$\mathcal{H} = \sum_i \left(\tfrac{1}{2}\pi_i^2 + \tfrac{1}{2}(\phi_i - \phi_{i+1})^2 + \tfrac{1}{2}\phi_i^2 + g\phi_i^4\right) \tag{1}$$

with the canonical commutation relations $[\phi_i, \pi_j] = \mathrm{i}\delta_{ij}, [\phi_i, \phi_j] = 0$ and $[\pi_i, \pi_j] = 0$. Note that for $g < 0$, the potential is not bounded below and renders the state $\phi \approx 0$ unstable (false vacuum). The decay rate due to quantum fluctuations is our concern. We will show that in contrast to 0 + 1 dimension mentioned above, the decay rate is *enhanced* owing to inter-instanton interaction.

The present paper is organized as follows. In section 2, we calculate the decay rate by means of the strong-coupling expansion. We explain the methodological details, and check the validity by means of an alternative simulation. In the last section, we summarize the present paper.

2. Results and discussions

In this section, we will calculate the false-vacuum decay rate of the model (1) through the strong-coupling expansion. To begin with, we will formulate the basis of the expansion.

2.1. Strong-coupling expansion

Making use of the rescalings $\phi \to g^{-1/6}\phi$ and $\pi \to g^{1/6}\pi$, we arrive at the expression,

$$\mathcal{H} = g^{1/3}\, h \tag{2}$$

where

$$h = \sum_i \left(\tfrac{1}{2}\pi_i^2 + \phi_i^4 + \frac{1}{g^{2/3}} \left(\tfrac{1}{2}(\phi_i - \phi_{i+1})^2 + \tfrac{1}{2}\phi_i^2 \right) \right). \tag{3}$$

According to the formula, the quadratic potential terms are regarded as perturbations, and so the ground-state energy is expanded in terms of the strong-coupling parameter $\lambda = 1/g^{2/3}$;

$$E_{\mathrm{g}} = g^{1/3}\, e_{\mathrm{g}} \tag{4}$$

where

$$e_{\mathrm{g}} = \sum_{n=0} a_n\, \lambda^n. \tag{5}$$

Note that the unperturbed Hamiltonian $h|_{\lambda=0}$ is biquadratic. Hence, it is not quite straightforward to perform perturbations with respect to this limit. Here, however, we will manage the perturbation expansion with the aid of computer calculations.

2.2. Linked-cluster expansion

The unperturbed Hamiltonian is a collection of independent anharmonic oscillators and the perturbation introduces coupling among them. In such cases, the linked-cluster expansion is useful to generate perturbation series. The linked-cluster expansion is a method of, so to speak, computer-aided diagrammatic expansion [8–10]. To perform cluster expansion, we should nevertheless set up unperturbed eigensystems. For that purpose, we must diagonalize the Hamiltonian of each local anharmonic oscillator $h_i = \pi_i^2/2 + \phi_i^4$. We carried out the diagonalization in the following way. (a) An oscillator spans infinite-dimensional Hilbert space. In order to perform a computer simulation, we need to restrict the number of bases. For that purpose, we prepare low-lying $M = 400$ states of a *harmonic* oscillator with quadratic potential $\Omega^2\phi^2/2$, namely, $\{|n\rangle_\Omega\}$ $(n = 0, \ldots, M-1)$. Note that the diagonalization of h_i is now manageable, because the Hilbert space is spanned by the finite number of bases just prepared. Here, Ω is a freely tunable variational parameter and we adjust it so as to minimize ${}_\Omega\langle 0|h_i|0\rangle_\Omega$, namely, we choose $\Omega = 6^{1/3}$. (This idea is reminiscent of Feynman and Kleinert [15], who calculated the thermodynamics of an anharmonic oscillator by replacing the biquadratic potential with an optimal quadratic one.) (b) With respect to the Hilbert-space frame $\{|n\rangle_\Omega\}$ $(n = 0\text{–}M-1)$, we represented the anharmonic-oscillator Hamiltonian h_i and diagonalized it to obtain the energy levels and the eigenvectors. (c) Provided that those eigenvectors are at hand, we carry out secondary Hilbert-space truncation: we extract m low-lying eigenvectors among M and discard the others. Henceforth, those m vectors are to be used to span the (intra-oscillator) Hilbert space. (Such a Hilbert-space restriction scheme originates in Wilson, who diagonalized a huge cluster of conduction electrons [16].)

To summarize, we truncated the intra-oscillator bases through two steps. First, we utilized the eigenvectors of a *harmonic* oscillator to span the Hilbert-space frame. Those were not very efficient, and so we prepared a rather huge number of $M = 400$ bases in practice. In that sense, the second truncation was significant, where we retained only m low-lying bases after solving the eigensystems of the intra-site Hamiltonian h_i. These bases turned out to be very efficient (see below), and only $m = 10$–25 bases are necessary so as to achieve reliable calculations in

the succeeding linked-cluster expansion. (Note that to perform the linked-cluster expansion, we need to store, in computer memory, huge Hilbert-space vectors for clusters consisting of *many* oscillators.)

Before going into the cluster expansion, we will check the reliability of the Hilbert-space restrictions. We treat a single anharmonic oscillator (namely, we ignore the inter-oscillator coupling) with respect to the restricted Hilbert space mentioned above. We used the ordinary Rayleigh–Schrödinger perturbation theory, because the system is a one-body problem. The strong-coupling perturbation coefficients are reported in the literature [17]. We observed the following encouraging features. First, the choice of $M = 400$ is sufficient. Namely, it reaches the limit of numerical round-off error (we used an extended precision of 16-byte real number) and further increase of M just alters the final few digits. Secondly, we found that rather small m yields precise data. For example, $m = 15$, which would seem exceedingly small, reproduces the perturbation coefficients reported in [17] with a high precision of order $\sim 10^{-17}$ (that is not relative but absolute error). Moreover, the precision is maintained even for high-order perturbation coefficients. For example, the choice of $M = 400$ and $m = 25$, for which the simulation takes ten minutes or so, is sufficient to reproduce the full result of [17].

Encouraged by these findings, we performed the linked-cluster expansion for the lattice ϕ^4 model (3). We obtained the perturbation series up to 11th order. The strong-coupling series is given by,

$$\begin{aligned} e_{\mathrm{g}} = {} & 0.667\,986\,259\,155\,777\,108\,270\,962\,016\,88 \\ & + 0.431\,006\,350\,142\,594\,730\,060\,957\,382\,75\lambda \\ & - 0.101\,488\,095\,211\,118\,632\,941\,259\,445\,02\lambda^2 \\ & + 0.048\,038\,456\,464\,436\,374\,420\,347\,753\,41\lambda^3 \\ & - 0.029\,018\,513\,979\,643\,624\,653\,232\,757\,064\lambda^4 \\ & + 0.019\,777\,791\,330\,895\,673\,863\,274\,529\,570\lambda^5 \\ & - 0.014\,454\,753\,622\,894\,705\,466\,341\,917\,665\lambda^6 \\ & + 0.011\,061\,391\,245\,982\,279\,114\,094\,315\,86\lambda^7 \\ & - 0.008\,749\,346\,526\,9972\lambda^8 \\ & + 0.007\,096\,747\,591\,805\lambda^9 \\ & - 0.005\,871\,428\lambda^{10} + 0.004\,936\,22\lambda^{11} \end{aligned} \tag{6}$$

with uncertainties only in the final digits.

2.3. Resummation and its verification with DMRG

In the above, we obtained strong-coupling series expansion for e_{g} (6). We plotted the result in figure 1. We truncated the series at various orders, which are indicated for the respective curves. We see that the curves start to deviate at $\lambda \approx 1$ and higher order data exhibit even worse convergence. Hence, it is suggested that the series (6) has finite convergence radius $|\lambda| \sim 1$. In order to go beyond the convergence bound and extract meaningful physics, we have to process our data with some resummation trick.

We found that Aitken's δ^2-process [18],

$$S'_n = S_n - \frac{(S_n - S_m)^2}{S_n - 2S_m + S_l} \tag{7}$$

is very useful to accelerate the convergence of our series. Here, S_l, S_m and S_n are three successive partial sums truncated at the respective orders. We plotted the resummed results in

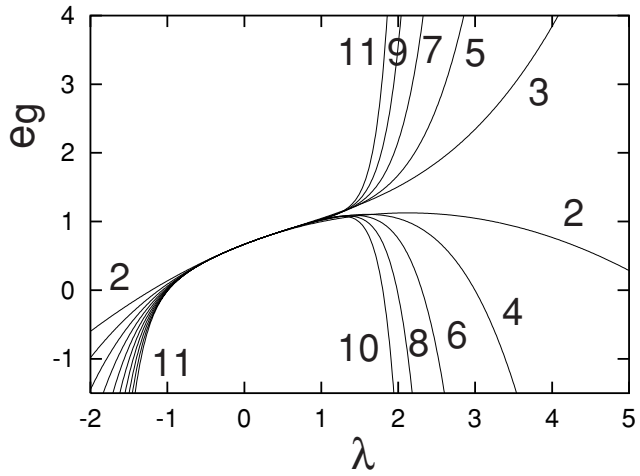

Figure 1. Strong-coupling series $e_g(\lambda)$ (6) is plotted. The series is truncated at various orders. A sudden deviation may indicate the convergence bound. Convergence-accelerated data are presented in figure 2.

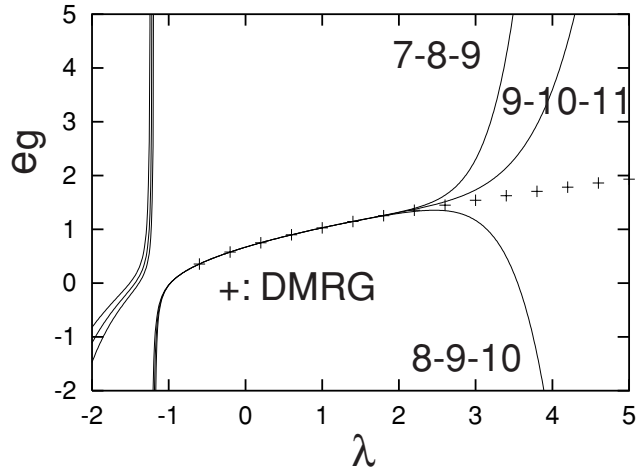

Figure 2. The same as figure 1, but the data are convergence-accelerated by formula (7). A symbol such as *l-m-n* indicates that the data are processed using the three partial sums S_l, S_m and S_n. We also present a first-principle simulation result by means of the density-matrix renormalization group. We confirm that our series achieves good convergence over the range $\lambda < 2$.

figure 2. A symbol such as 5-6-7 indicates that the data are accelerated with the partial sums of S_5, S_6 and S_7. We see that the data exhibit pronounced convergence improvement. Our data may be valid up to $\lambda \approx 2$.

In order to check the convergence bound more definitely, we performed an alternative first-principles simulation with the density-matrix renormalization group. Our algorithm is standard. For a comprehensive overview of this algorithm, interested readers may consult [19]. A full account of the technical details specific to the (1 + 1)-dimensional scalar field theory will be found in our paper [20]. (In this paper, we studied field ϕ confined within the

rigid-wall potential $V(\phi)$. In order to match the present case, one has to replace $V(\phi)$ with ϕ^4.) The numerical error was checked thoroughly in [20] and it was found to reach 10^{-7}. We monitored the performance in the present case as well and found that the precision was maintained. The error would be far less than the symbol size shown in the plot 2.

The first-principles data are shown in figure 2 as well. We see that our resummed data are valid up to $\lambda \approx 2$ fairly definitely.

Finally, we mention a singularity occurring at $\lambda \approx -2(<0)$; see figure 2. It is noteworthy that for $\lambda < 0$, the potential becomes of double-well form. Therefore, at a certain critical λ, there would be an Ising-type phase transition. The singularity found in our data may indicate the onset of the transition. Determination of the critical point for the lattice ϕ^4 model is attracting considerable attention recently in the context of the quantum ferroelectric transition [21]. We will pursue this issue elsewhere and in the present paper, we will not go into any further details.

2.4. Analytic continuation to $g < 0$: false-vacuum decay rate

In the above, we attained good convergence of the series expansion (6) with the aid of the convergence-acceleration trick (7). Armed by this achievement, in this subsection, we access the domain of $g < 0$ through the analytic continuation $g \to -g$. For $g < 0$, the potential is not bounded below and exhibits a local potential minimum in the vicinity of $\phi = 0$ (metastability). Because the series expansion (6) is an irrational function in terms of g, the analytic continuation renders an imaginary part in the ground-state energy. Thereby, from it, we can read off the false-vacuum decay rate. In practice, the analytic continuation is done through the path $g\exp(\mathrm{i}\theta)$ of $\theta = 0 \to \pi$. That is, the term $g^{1/3}$ gives rise to the contribution $g/2 + \mathrm{i}\sqrt{3}g/2$ after $g \to -g$.

So far, to calculate the decay rate, the instanton technique is used. The technique is justified for sufficiently large potential barrier (small g). In the following we will show that our series-expansion approach covers the instanton theory.

In figure 3, we plotted the false-vacuum decay rate multiplied by g, namely, $g\,\mathrm{Im}\,E_{\mathrm{g}}(-g)$, against $1/g$. The factor g should kill the prefactor of a dominant exponential contribution. That is, the instanton theory predicts that the decay rate should obey the formula,

$$\mathrm{Im}\,E_{\mathrm{g}}(-g) \propto \tfrac{1}{g}\exp(-S/g) \tag{8}$$

where S denotes the Euclidean action of one instanton. We solved the instanton solution numerically and obtained the estimate,

$$S = 1.189\,1027(5). \tag{9}$$

To be concrete, we will sketch the calculation method. First of all, one must reformulate the Hamiltonian formalism (1) into the Lagrangian formalism in the Euclidean spacetime. Thereby, we considered the system with 28 sites and imaginary time $\beta = 28$. The imaginary time is discretized into 8000 intermediate time slices. (Note that now the field is defined in the discretized spacetime.) Because the instanton solution (field configuration) should minimize the Euclidean action, the problem reduces to the minimization of a multi-dimensional function. That computation is readily achieved by the utilities supplied in simulation guide books such as [18]. The amount of error is estimated by changing the system sizes and discretization intervals.

We would like to draw the reader's attention to the fact that the formula (8) has an essential singularity at $g = 0$. That is why we selected the strategy of approaching from $g \to \infty$ rather than from $g = 0$.

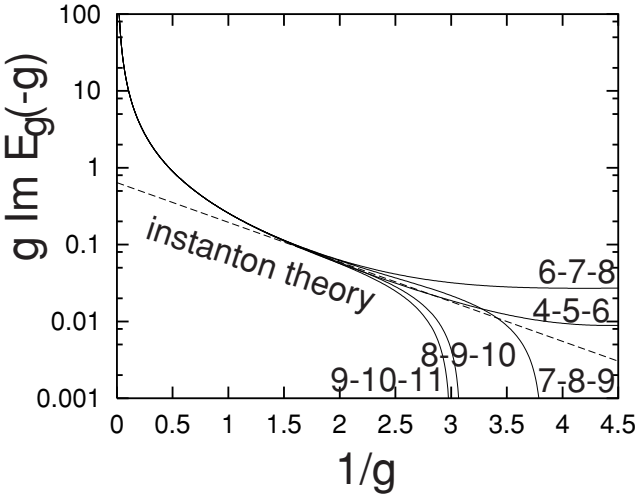

Figure 3. The false-vacuum decay rate (multiplied by g) $g\,\mathrm{Im}\,E_{\mathrm{g}}(-g)$ is plotted. The symbol *l-m-n* indicates that the data are convergence-accelerated by the use of three partial sums S_l, S_m and S_n. We plotted a slope $\exp(-S/g)$ which is predicted by the instanton theory; see text. Note that the instanton treatment is justified for large $1/g$. As a matter of fact, our series expansion obeys the prediction for $1/g > 1$. For $1/g < 1$, in contrast, our result exhibits notable enhancement. Hence, it is suggested that the inter-instanton interaction rather *enhances* the relaxation.

Let us turn to the discussion of our result of figure 3. As mentioned above, the instanton result (8) is validated for large $1/g$. As a matter of fact, for $1/g > 1$, our data approach the instanton prediction; we have drawn the slope of (8). In this respect, the convergence-acceleration trick (7) is crucial in our study, because it enables us to attain good convergence up to $1/g \sim 3$, which appears to reach the instanton region

For $1/g < 1$, on the other hand, our data indicate rapid enhancement of the decay rate, namely, the curve starts to deviate from the instanton prediction. It is to be stressed that our treatment is justified for the strong-coupling limit ($1/g \ll 1$). Therefore, it is found that the inter-instanton correlation gives rise to *enhancement* of relaxation. This feature is to be contrasted with that of 0 + 1 dimension, where the inter-instanton correlation results in *suppression* of the decay rate. Enhancement in 1 + 1 dimensions was speculated in the former study [13], where the authors utilized the *weak*-coupling expansion and the Borel technique. Although their series does not show any indication of convergence, their result actually captures a signal of relaxation enhancement.

According to Kleinert, in the regime $g \gg 1$, the decay process is governed by 'sliding' rather than instanton theory [22]. Nevertheless, we stress that the present series-expansion approach covers both instanton ($1/g > 1$) and sliding ($1/g < 1$) regimes in a unified way. Moreover, our series is readily improved systematically just by performing further cluster expansion.

In the above, we found that at $1/g \approx 1$, there exists a crossover boundary separating two distinctive regimes. Our result supports the previous proposal of [13]. The authors calculated the effective potential and found that for $g > 1.17$, the potential barrier is smeared out by quantum fluctuations. Their criterion would be sensible for separating instanton and sliding phases.

In figure 3, we see that the data of 9-10-11 and 8-9-10 show poor convergence. That may possibly be due to the fact that our 10th and 11th perturbation coefficients have rather few significant figures available.

Finally, we recollect past findings for the ϕ^4 theory in *continuous* spacetime. Brézin and Parisi completed the instanton calculation and obtained the formula $\mathrm{Im}\, E_{\mathrm{g}}(-g) = (0.081\ 5435/g)\ \exp(-1.462\ 6121/g)$ [23]. We notice that the instanton action is similar to that of our lattice model. Perhaps the decay process would be identical between the lattice model and the continuous-field theory.

3. Summary and discussions

So far, several *ab initio* approaches have been proposed in order to calculate the decay rate beyond the semiclassical approximation. In particular, the ϕ^4 model in 0 + 1 dimension has come under thorough investigation [11–14], while the extension to the many-body case remains unsuccessful. In the present paper, by means of the strong-coupling expansion, we studied the (1 + 1)-dimensional lattice ϕ^4 model (1). We demonstrated that the linked-cluster expansion method works very efficiently, provided that the Hilbert-space restriction is processed properly. In addition, we found that the convergence-acceleration trick (7) is significant. In fact, the convergence-accelerated sum reproduces the first-principle data for a considerably wide range $\lambda < 2$.

Based on the above achievements, we surveyed the domain of metastability through the analytic continuation $g \to -g$. We are concerned about the false-vacuum decay rate $\mathrm{Im}\, E_{\mathrm{g}}(-g)$; see figure 3. Our result indicates that there are two regimes. For $g < 1$, our result obeys the prediction by the instanton theory. It is to be stressed that the convergence acceleration (7) is significant to reach the instanton regime. For shallow potential barrier $g > 1$, the relaxation is no longer described by an instanton, but the relaxation rate acquires notable enhancement. According to Kleinert, for $g > 1$, the relaxation is driven by sliding rather than instanton theory. Nevertheless, we stress that our series-expansion approach does cover both regions with a unified framework, and it is readily improved systematically just by continuing the perturbation further. It is promising that the present method might be applied to other wide classes of metastable systems.

As mentioned above, we also performed the density-matrix-renormalization-group simulation. From the simulation data, we are able to extract perturbation coefficients by polynomial fitting. This technique is applicable to those models that even possess complicated interactions and spatial inhomogeneity. Tunnelling phenomena assisted by an impurity is of current interest [24]. However, ambiguities in estimating fitting errors are not fully resolved at present. This is left for future study.

References

[1] Langer J S 1967 *Ann. Phys., NY* **41** 108
[2] Coleman S 1985 *Aspects of Symmetry* (Cambridge: Cambridge University Press)
[3] Fisher M E 1967 *Physics* **3** 255
[4] Günther N J, Nicole D A and Wallace D J 1980 *J. Phys. A: Math. Gen.* **13** 1755
[5] Günther C C A, Rikvold P A and Novotny M A 1994 *Physica* A **212** 194
[6] Stoll E P and Schneider T 1977 *Physica* B **86–88** 1419
[7] Rikvold P A, Tomita H, Miyashita S and Sides S W 1994 *Phys. Rev.* E **49** 5080
[8] Marland L G 1981 *J. Phys. A: Math. Gen.* **14** 2047
[9] Hamer C J and Irving A C 1984 *J. Phys. A: Math. Gen.* **17** 1649
[10] Singh R R P, Gelfand M P and Huse D A 1988 *Phys. Rev. Lett.* **61** 2484
[11] Drummond J E 1982 *J. Phys. A: Math. Gen.* **15** 2321
[12] Suzuki H and Yasuta H 1997 *Phys. Lett.* B **400** 341
[13] Suzuki H and Yasuta H 1998 *Phys. Rev.* D **57** 2500
[14] Karrlein R and Kleinert H 1994 *Phys. Lett.* A **187** 133

[15] Feynman R P and Kleinert H 1986 *Phys. Rev.* A **34** 5080
[16] Wilson K 1975 *Rev. Mod. Phys.* **47** 773
[17] Janke W and Kleinert H 1995 *Phys. Rev. Lett.* **75** 2787
[18] Press W H, Teukolsky S A, Vetterling W T and Flannery B P (ed) 1992 *Numerical Recipes in FORTRAN: The Art of Scientific Computing* (Cambridge: Cambridfe University Press)
[19] Peschel I, Wang X, Kaulke M and Hallberg K (ed) 1999 *Density-Matrix Renormalization—A New Numerical Method in Physics* (Berlin: Springer)
[20] Nishiyama Y 2001 *Phys. Rev.* B **64** 064510
[21] Rubtsov A N and Janssen T 2001 *Phys. Rev.* B **63** 172101
[22] Kleinert H 1993 *Phys. Lett.* B **300** 261
[23] Brézin E and Parisi G 1978 *J. Stat. Phys.* **19** 269
[24] Kato T 2000 *J. Phys. Soc. Japan* **69** 2735